Supplementary Materials

Self-Assembled A-D-A Type Indacenodithiophene-based Small Conjugated Molecule/TiO_2 for Enhancing the Photocatalytic Activity

Enwei Zhu [a,b], Tingyu Yang[c], Juan Du[a, b], Chunbo Liu[c,*], Chunhong Ma[c,*], Haiyong Guo[d,*]

[a] *Key Laboratory of Preparation and Applications of Environmental Friendly Materials, Jilin Normal University, Ministry of Education, Changchun 130103, P.R. China*

[b] *College of Chemistry, Jilin Normal University, Siping 136000, P.R. China*

[c] *College of Engineering, Jilin Normal University, Siping 136000, P.R. China*

[d] *Department of Biological Science, School of Life Science, Jilin Normal University, Siping 136000, P.R. China*

Corresponding Author

* Email:chunboliu@jlnu.edu.cn; jlspmch@163.com; guohaiyong78@jlnu.edu.cn;

Chemicals

4,9-dihydro-4,4,9,9-tetraoctyl-s-indaceno[1,2-b:5,6-b']dithiophene (IDT), 2-cyanoacetic acid, ammonium acetate, acetic acid was supplied by Jiaxing Hepu Optoelectronics Technology Co., Ltd. (Zhejiang, China). TiO_2 was supplied by Energy Chemical (Shanghai, China). Nitrogen gas (N_2) was purchased from Siping Hongyuan Gas Co., Ltd. (Siping, China). Phosphate buffered saline (PBS) (pH = 7.2) was supplied by Beijing Solarbio Science & Technology Co., Ltd. (Beijing, China). Tryptic soy agar (TSA) and tryptic soy broth (TSB) were supplied by Qingdao Hope Bio-Technology Co., Ltd. (Qingdao, China). Isopropanol was purchased from Tianjin Fuyu Co., Ltd. (Tianjin, China). Propidium iodide (PI) and SYTO-9 were supplied by Invitrogen (American). Ethylenediamine tetraacetic acid disodium salt (EDTA-2Na) was supplied by Changchun Tianjia Biological Techonogy Co., Ltd. (Changchun, China). Methanol, tetrahydrofuran (THF), acetic acid, toluene, hexane, $K_2Cr_2O_7$, NaN_3 and L-Ascorbic acid were supplied by Sinopharm Chemical Reagent Beijing Co., Ltd. (Beijing, China). NIH3T3 cells were purchased from Huake Cell Biotechnology (Beijing, China). 4-hydroxy-2,2,6,6-tetramethyl-1-piperidine (TEPM) were obtained from Sigma-Aldrich. 5,5-dimethyl-1-pyrroline N-oxide (DMPO) and 3,4-Dihydro-2-methyl- 1,1-dimethylethyl ester-2H-pyrrole-2-carboxylic acid-1-oxide (BMPO) were obtained from DOJINDO (Japan). Cell Counting Kit-8 (CCK-8), fetal bovine serum (FBS) and Dulbecco′s modified eagle medium (DEME) were supplied by HyClone (USA), PEAK SERUM (USA) and MCE (USA), respectively. The water used in all experiments was deionized (DI).

Preparation of the **bulk g-C_3N_4 (**bg-C_3N_4). The bg-C_3N_4 was prepared by the thermal polymerization process. Typically, 1 g of urea was transferred into a 50 mL alumina crucible with a cover, and then heated at 550 ℃ for 4 h with a heating rate of 5 ℃ min^{-1} under air atmosphere. After cooling to room temperature, the yellow products were milled into powder and collected for further characterization.

Photocatalytic degradation experiments

The photocatalytic activities of TiO_2, IDT-COOH and IDT-COOH/TiO_2 with varying IDT-COOH mass ratio were evaluated by degrading TC under visible light irradiation ($\lambda > 420$ nm). A 250W xenon lamp with a cut-off filter UV light ($\lambda < 420$ nm) was employed as the visible light source and the average light intensity of 80 mW cm^{-2} was fixed. In detail, 16 mg of the

photocatalyst was dispersed into the 40 mL aqueous solution of TC (20 mg L^{-1}). The suspension solution was stirred in the dark for 1 h before irradiation to keep the adsorption-desorption equilibrium. At intervals of 30 min, aliquots of 3 mL were withdrawn and centrifuged. The concentrations of TC were detected by a UV-2550 spectrometer and the detection wavelength of TC was 357 nm. TOC were measured on a multi N/C 2100 (AnalytikJena AG, Germany) TOC analyzer.

Photocatalytic degradation pathway of tetracycline by IDT-COOH/TiO_2

Intermediate products obtained during photodegradation of TC over IDT-COOH/TiO_2 with visible light illumination were studied by HPLC-MS (HPLC: Agilent1100, China; MS: TSQ quantum Ultra, America). The intermediates with *m*/*z* = 461, 477, 449 and 309 were produced during photodegradation of TC under visible light illumination. Therefore, we can propose the TC photodegradation pathways (Fig. S10). The intermediate with *m*/z = 416 was produced after active radicals reacted with 1-(12, 13) double bond. Then, the 1-(2, 3) double bond of 2 structure was oxidized to form 3 (m/z =477) molecule, and then the 4 (m/z =449) molecule was produced in sequence by losing methyl groups. Further h^+ and $\cdot O_2^-$ attacked D to generate the 5 intermediate with m/z = 309 via decarboxylation reactions. Finally, through a series of open-ring reactions and the loss of functional groups, these small intermediate products were oxidized and decomposed into H_2O and CO_2.

Photocatalytic disinfection experiments

Photocatalytic disinfection performance of TiO_2, IDT-COOH and IDT-COOH/TiO_2 with varying IDT-COOH mass ratio was evaluated by inactivation of Gram-positive *S. aureus* (USA 300). Before test, all culture medium solution (TSA, TSB and PBS) and glassware were autoclaved at 121 ℃ for 30 min. First, *S. aureus* cells were cultured in TSB at 37 °C for 12 h and centrifuged to obtain ca. 10^8 colony forming units per milliliter (cfu mL^{-1}) in PBS. The photocatalytic disinfection experiments were conducted under a 250 W xenon arc lamp equipped with an optical cutoff filter (λ< 420 nm). The temperature was kept at 30 °C and the visible light intensity was fixed at 80 mW cm^{-2}. The concentration of *S. aureus* for antibacterial test was ca. 10^7 cfu mL^{-1}. At various illumination time intervals, 0.1 mL of tested sample was pipetted out, diluted by PBS serially and spread on TSA plates. Lastly, the cell numbers were counted to calculate the relative survival rate and cell density reduction of *S.*

aureus after incubation at 37 °C for 20 h. Dark control (*S. aureus* with 30% IDT-COOH/TiO_2) and light control (*S. aureus* without photocatalyst) were performed. All the tests were repeated for three times.

Rabbit plasma test

Staphylococcal coagulase is an important virulence factor for *S. aureus*. Coagulase converts host prothrombin to staphylothrombin, leading to activation of the protease activity of thrombin. It was predicted that coagulase could protect bacteria from phagocytic and immune defenses by causing localized clotting. The expression of coagulase of *S. aureus* was examined after the interaction between 30% IDT-COOH/TiO_2 and the bacteria. A tube coagulation assay based on freeze-dried rabbit plasma was performed. 30% IDT-COOH/TiO_2 (8 mg) was added to bacteria culture (20 mL) and allowed to react for 0, 0.5, 1, 1.5 and 2 h. Then 800 μL of reaction solution collected at different times were added to 500 μL of rabbit plasma in small ampules of glass tubes. The mixture samples were incubated at 37 °C for 6 h, and rabbit plasma coagulation was examined.

Fluorescence microscopy observation of bacteria

Furthermore, Fluorescent-based cell live/dead tests were carried out to explore the integrity of bacterial cell membranes. In brief, the bacterial liquids before and after 2 h irradiation treatment in the control and experimental groups were collected and centrifuged at 8000 rpm for 2 min with the supernatant being discarded. The obtained bacteria were dispersed in 50 μL sterile PBS solution and stained with 25 μL of SYTO-9 (6 mg mL^{-1} in sterilized deionized water) and 25 μL of PI (6 mg mL^{-1} in sterilized deionized water) solution for 15 min in the dark at room temperature. Lastly, 10 μL of stained bacterial liquid was taken out and dropped on the center of slide and then imaged using a laser scanning confocal microscope (Nikon Ti-s, Japan).

Growth studies

The *S. aureus* was used for the growth studies against 30% IDT-COOH/TiO_2. 8 mg 30% IDT-COOH/TiO_2 was dispersed in 20 mL of TSB solution in a 120 mL self-designed glass jacketed reactor containing bacteria solution (10^7 cfu mL^{-1}). Aliquots were taken after every 2 h, 100 μL tested suspension sample was pipetted out and serially diluted using PBS and spread on nutrient TSA plates. After incubation at 37 ℃ for 18 h, the cell densities were checked to determine the survival bacterial numbers. The growth curves were plotted

accordingly. Samples without treatment of IDT-COOH were used as light control. The reaction was carried out in a GHX-3 photochemical reaction instrument equipped with a 250 W xenon arc lamp and an optical cutoff filter (λ<420 nm). The visible light intensity was fixed at 80 mW cm^{-2}. The temperature was kept at 30 ℃ using a cryostatic tank.

Protein Leakage

Briefly, 10^7 cfu mL^{-1} of *S. aureus* was incubated with 30% IDT-COOH/TiO_2 (0.4 mg mL^{-1}) and exposed to visible light sources (GHX-3, 250 W xenon arc lamp) for 2 h. The bacteria solution without PBDT-F-COOH was the control group. The solution was centrifuged at 12000 rpm for 2 min at 4 °C. The supernatant liquid was transferred to a 96-well plate and the protein leakage concentrations were measured by the Enhanced BCA Protein Assay Kit (BL521A 500T, Biosharp, China) on a microplate reader.

Active species trapping experiments

In order to explore the active species produced in photocatalytic process, isopropanol (10 mmol L^{-1}), $K_2Cr_2O_7$ (2 mmol L^{-1}), L-ascorbic acid (2 mmol L^{-1}), NaN_3 (2 mmol L^{-1}) and EDTA-2Na (0.5 mmol L^{-1}), were employed as the traps of hydroxyl radicals (•OH), electrons (e^-), superoxide ($•O_2^-$), $^1O_2$ and holes (h^+), respectively. Electron spin resonance (ESR) analyses were performed on the Bruker EMX-Plus spectrometer with the concentration of spin traps of DMPO, BMPO and TEMP being 0.22 mmol L^{-1} in deionized water.

Cell Toxicity Assay

The CCK-8 assay (Huake biotech, beijing, China) was applied to study the cytotoxicity of the PBDT-F-COOH. First, the NIH3T3 cells were cultured with dulbecco′s modified eagle medium (DEME, HyClone) (6 mL) containing 1% penicillin-streptmycin solution (HyClone) and 10% fetal bovine serum (FBS, PEAK) in a humidified atmosphere containing 5% CO_2 at 37 °C. The cell culture medium was refreshed every 3 days. Then, then NIH3T3 cells (5×10^4 cells mL^{-1}) were cultured in DMEM (100 μL) for 24 h on a 96-well plate so that they adhered to the plate wall, 5 replicates per well. Afterwards, DMEM was discarded and fresh DMED medium containing IDT-COOH with different concentrations of 200 μg mL^{-1}, 400 μg mL^{-1} and 800 μg mL^{-1} was added in each well respectively. After 24 h co-cultivation, each well was incubated with 10 μL CCK-8 solution at 37 °C for 2 h, the absorbance at 450 nm was measured using *Multi*mode *Plate Reader*. No PBDT-F-COOH sample was added as control group. All experimental values are presented as means ±SD. The statistical significance of the

difference was performed by Two-way ANOVA and Student's *t*-test using Graph-Pad Prism 7.0 software. A *P*-value <0.05 indicates statistical significance.

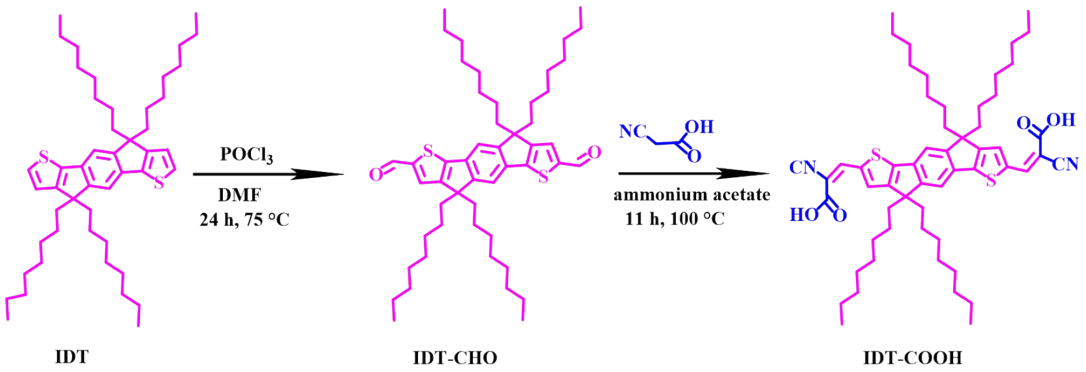

Scheme S1. The synthetic routes of IDT-COOH.

Fig. S1. Photographs of (a) amorphous IDT-COOH, (b) self-assembled IDT-COOH, (c) physically mixing 30% IDT-COOH/TiO_2, (d) 10% IDT-COOH/TiO_2, (e) 20% IDT-COOH/TiO_2, (f) 30% IDT-COOH/TiO_2 and (f) 40% IDT-COOH/TiO_2.

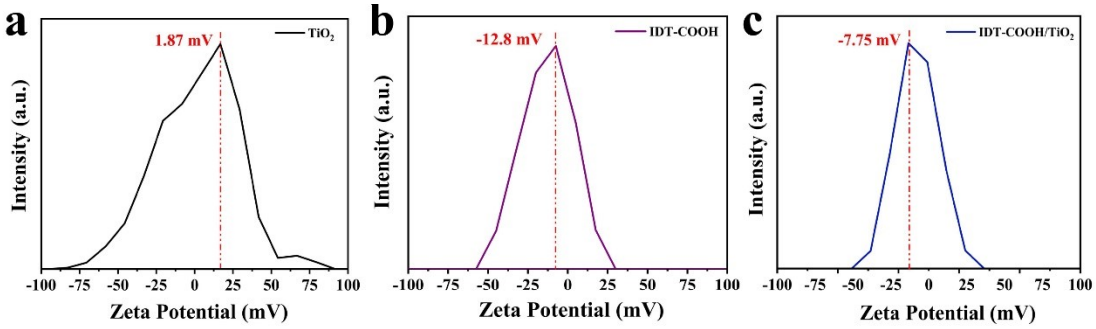

Fig. S2. Zeta potentials of (a) TiO_2, (b) IDT-COOH and (c) 30% IDT-COOH/TiO_2.

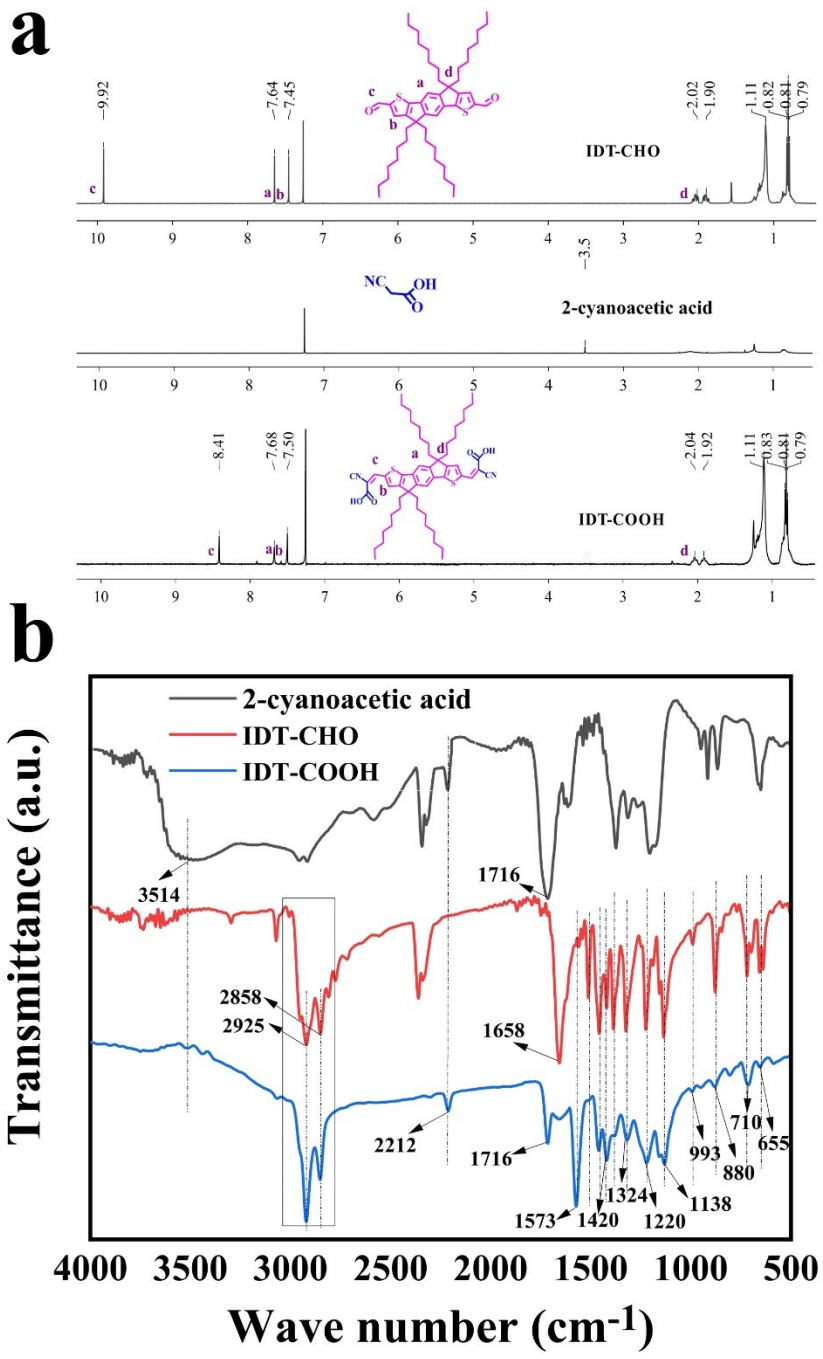

Fig. S3. (a) ^{1}H NMR and (b) FT-IR spectra of samples.

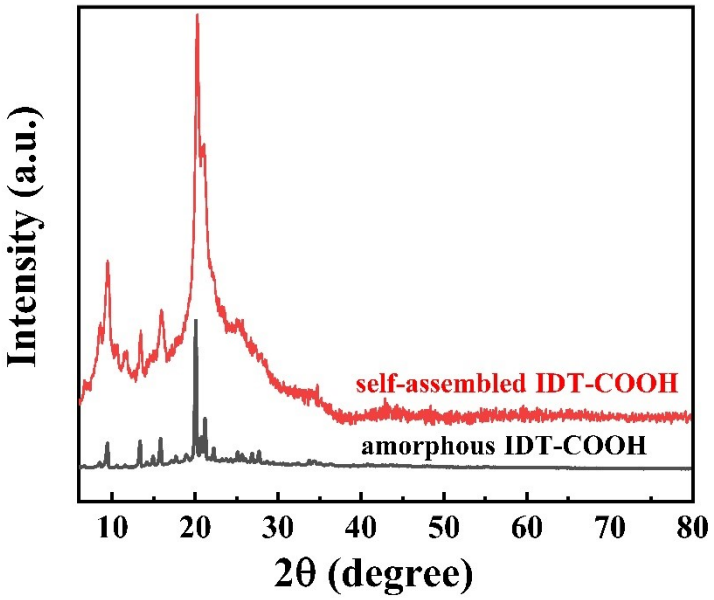

Fig. S4. XRD patterns of amorphous IDT-COOH and self-assembled IDT-COOH.

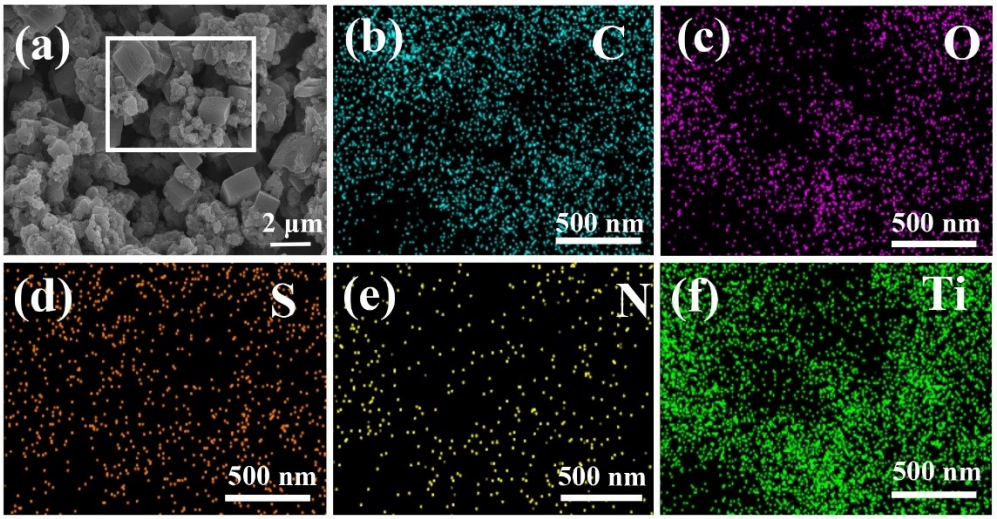

Fig. S5. SEM images of (a) IDT-COOH/TiO_2. The element mappings of (b) C, (c) O, (d) S, (e) N, (f) Ti.

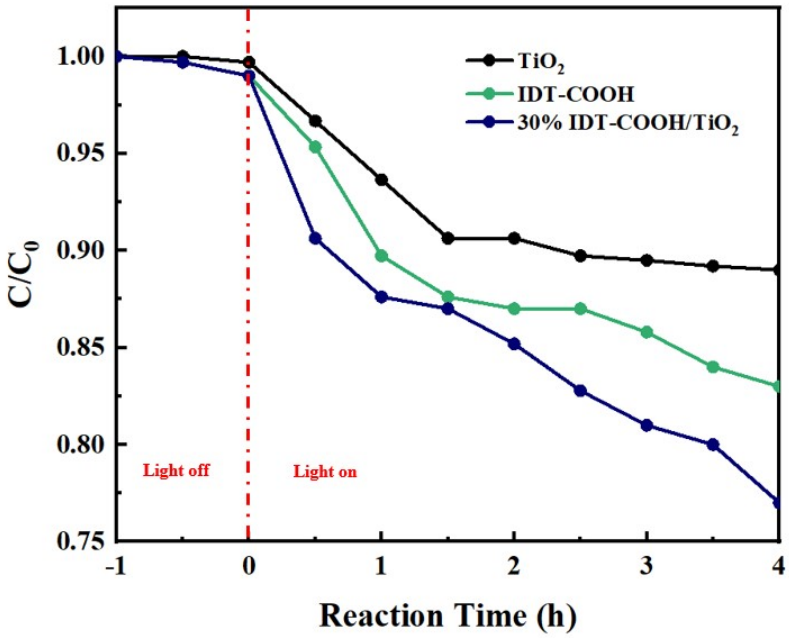

Fig. S6. Photodegradation toward BPA of TiO_2, IDT-COOH and 30% IDTCOOH/TiO_2

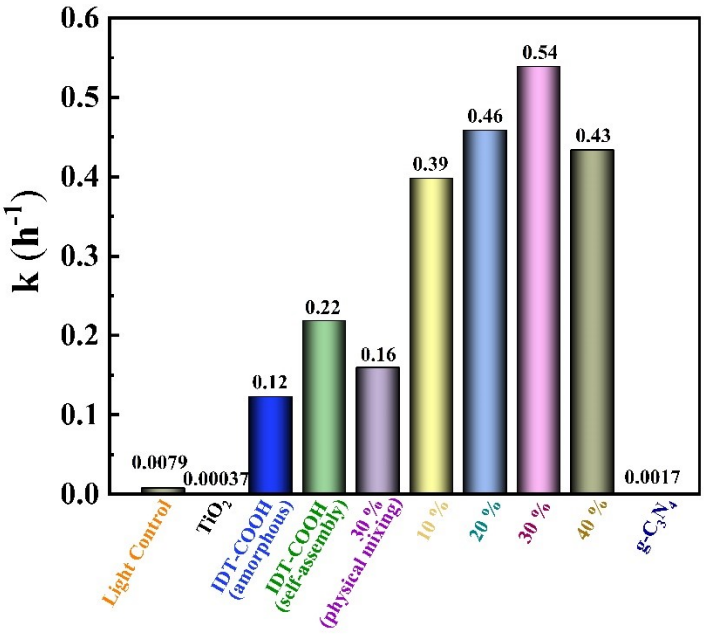

Fig. S7. Apparent rate constants *k* of samples for TC degradation.

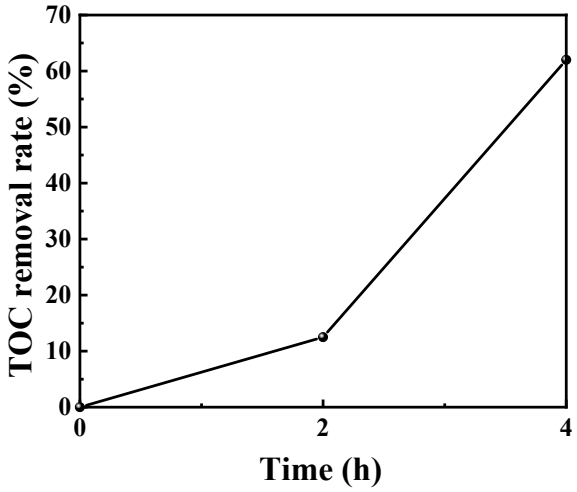

Fig. S8. TOC removal plots of TC over 30% IDT-COOH/TiO_2 under visible light irradiation.

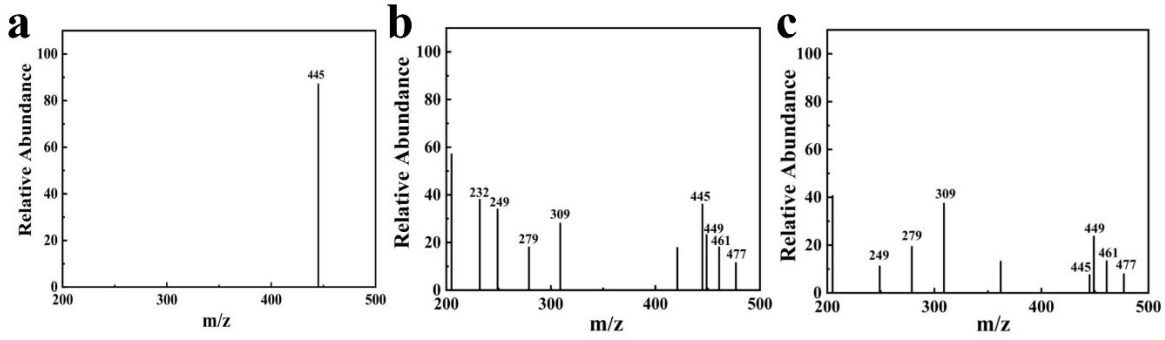

Fig. S9. HPLC-MS chromatograms of (a) TC and produced intermediates at (b) photodegradation reaction time 2 h and (c) 4 h.

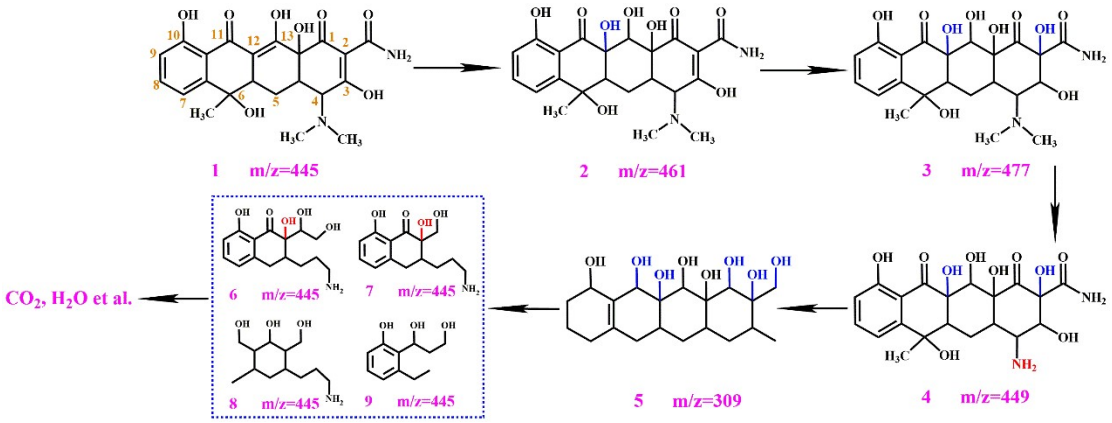

Fig. S10. Possible intermediate products (A-I) at the degradation process of TC over 30% IDT-COOH/TiO_2.

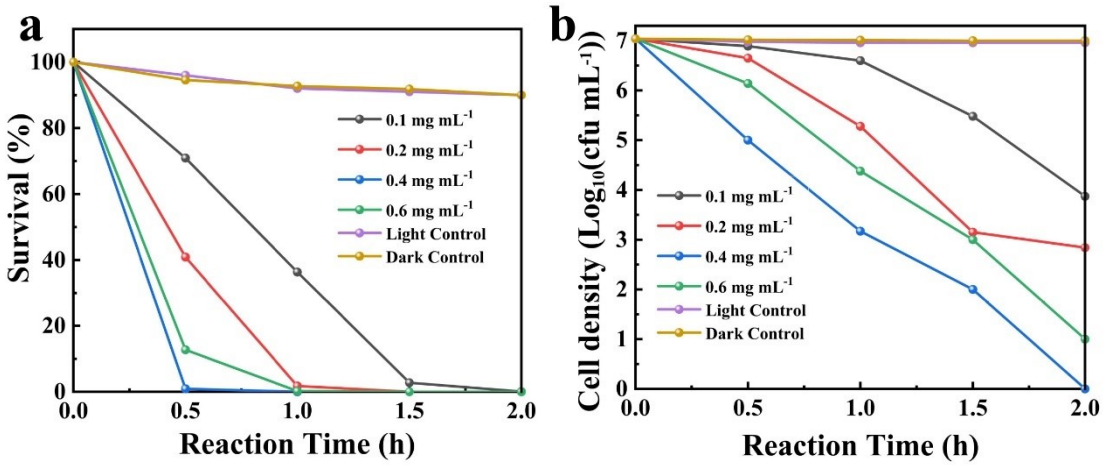

Fig. S11. Effect of 30% IDT-COOH/TiO_2 concentration on the photocatalytic inactivation of *S. aureus* (10^7 cfu mL^{-1}).

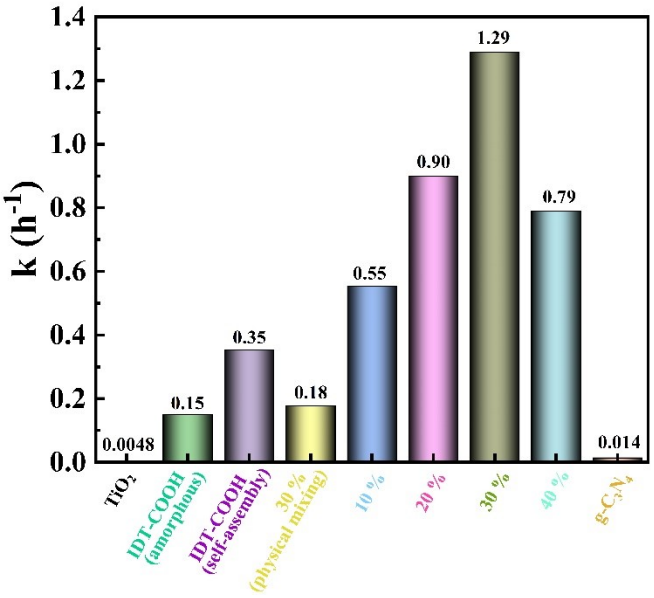

Fig. S12. Photocatalytic inactivation reaction rate constants (*k*) of samples against *S. aureus.*

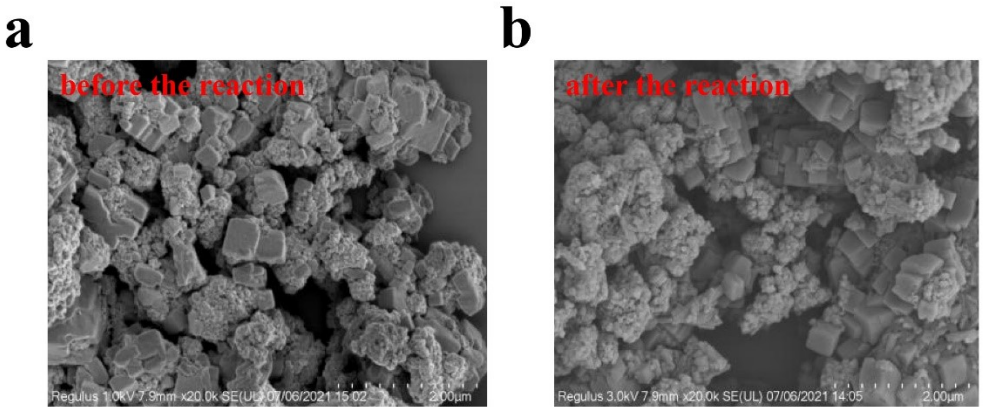

Fig. S13. SEM images of 30% IDT-COOH/TiO_2 (a) before and (b) after three runs.

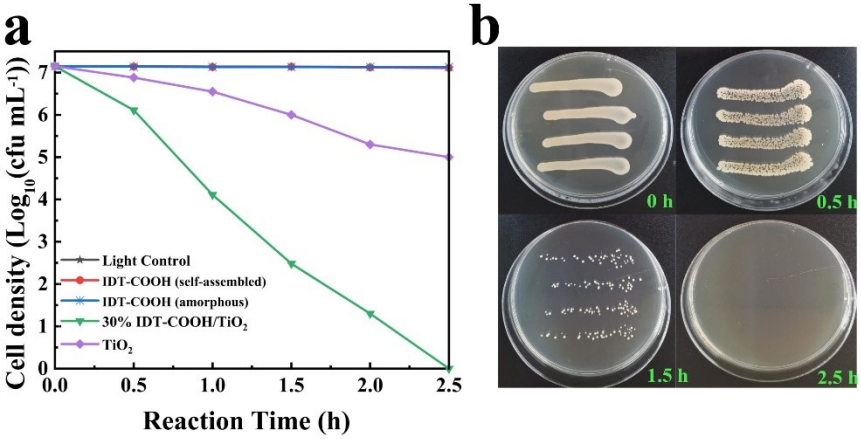

Fig. S14. Photocatalytic inactivation against *S. aureus* of TiO_2, amorphous IDT-COOH, self-assembled IDT-COOH and 30% IDT-COOH/TiO_2 (0.4 mg mL^{-1}) and images of colonies on an agar plate under sunlight illumination (Siping city of Jilin province, 10:00-13:00, December 1, 2021)

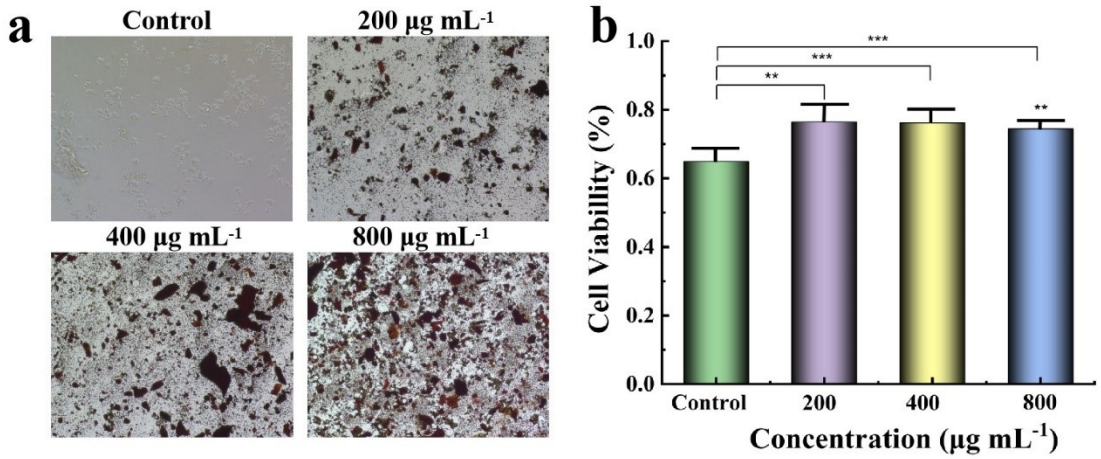

Fig. S15. (a) NIH3T3 cells images of cytotoxicity testing and (b) NIH3T3 cells viability after coculturing for 24 h with various concentrations of 30% IDT-COOH/TiO_2. The error bars indicate means ± SD (n = 3).

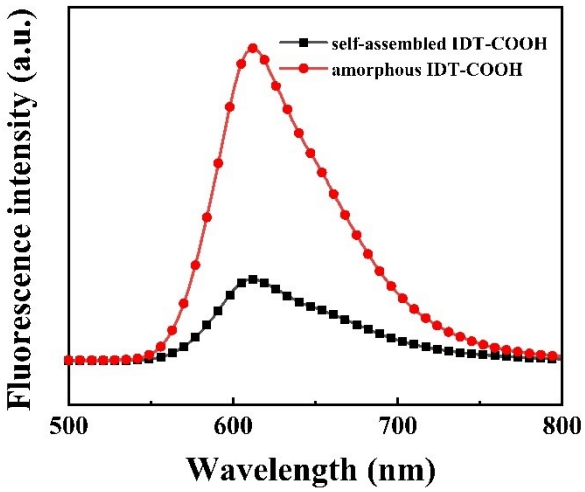

Fig. S16. Fluorescence spectra of self-assembly IDT-COOH and amorphous IDT-COOH.

Table S1. Representative Photocatalysts Based on Polythiophene (PTh)/TiO_2 with Their Concentration, Target Microorganisms, and Photocatalytic degradation Performances.

photocatalyst	concentration	light source	model pollutants	degradation efficiency	released year
P_3HT/TiO_2 [1]	0.005 mg mL^{-1}	UV	OG	~100% 1 h	2007
PTh/TNT [2]	1 mg mL^{-1}	visible light	2,3-DCP	51% 420 min	2009
TiO_2/P3HT [3]	film	visible light	MO	88.5% 10 h	2009
P3HT/TiO_2 [4]	1 mg mL^{-1}	visible light	MeO	decrease in absorbance of MeO 10 h	2010
Polythiophene /TiO_2 [5]	1 mg mL^{-1}	UV-visible	MO	85.6% 2 h	2010
PT/TiO_2 [6]	1 mg mL^{-1}	visible light	MeO	80.3% 10 h	2010
PTh/TiO_2 [7]	1 mg mL^{-1}	visible light	MO	95.1% 10 h	2010
PTh/TiO_2[8]	1 mg mL^{-1}	visible light	RhB	98% 10 h	2011
P3HT/TiO_2 [9]	1 mg mL^{-1}	visible light	MO	96% 10 h	2012
TiO_2-Mt/PTP-SDS [10]	0. 5 mg mL^{-1}	visible light	RhB	74.3% 1 h	2013
mTiO_2-P3HT [11]	coating	visible light	MO	~50% 3 h	2013
PTh/TiO_2 [12]	1 mg mL^{-1}	UV	Phenol	45% 2 h	2013
PProDOT/TiO_2 [13]	0.4 mg mL^{-1}	sunlight	MB	79.6% 7 h	2014
PProDOT-Me_2/TiO_2 [13]	0.4 mg mL^{-1}	sunlight	MB	62.8% 7 h	2014
poly(TPT)/TiO_2 [13]	0.4 mg mL^{-1}	sunlight	MB	90.5% 7 h	2014
poly(TMPT)/TiO_2 [13]	0.4 mg mL^{-1}	sunlight	MB	84.6% 7 h	2014
TiO_2-Cu/PTh [14]	0. 6 mg mL^{-1}	visible light	RhB	~100% 1.3 h	2015
Sn-TiO_2/PTh [15]	0. 4 mg mL^{-1}	visible light	NB	99.4% 1.75 h	2015
PTh-rGO-TiO_2 [16]	0.25 mg mL^{-1}	visible light	MB	63% 2 h	2016
FeTCPP–TDI–TiO_2 [17]	1 mg mL^{-1}	visible light	TC	99.2% 2 h	2016
Cu-TiO_2/polythiophene [18]	0.6 mg mL^{-1}	visible light	RhB	99.4% 1.25 h	2017
PTh/Sn-TiO_2 [19]	0.6 mg mL^{-1}	visible light	CR	95% 2 h	2017
CT-g-ZnTAPc-2 [20]	0.5 mg mL^{-1}	visible light	TC·HCl	~100% 1.7 h	2020
PTh/TiO_2-P90 [21]	0.5 mg mL^{-1}	UV	MeO	98% 2.42 h	2021
FSTZP[22]	0.3 mg mL^{-1}	visible light	TC·HCl	86% 1 h	2021
IDT-COOH/TiO_2 (this work)	0.4 mg mL^{-1}	visible light	TC	92.5% 4 h	

Table S2. Representative Photocatalysts Based on Organic Conjugated Molecules/TiO_2 with Their Concentration, Target Microorganisms, and Photocatalytic Disinfection Performances Under Visible Light

photocatalyst	concentration	bacteria	photocatalytic performance	released year	publication
ZnPc-TiO_2 [23]	solution	*S. aureus*	80% inactivation 0.5 h	2010	Laser Phys. Lett.
MF_2POH@TiO_2 [24]	100 mg mL^{-1}	*S. aureus*	7 log inactivation 2 h	2010	Catal. Today
PANI-TiO_2 [25]	0.1 mg mL^{-1}	*E. coli*	strong inhibition	2014	Chem. Eng. J.
quercetin-TiO_2 [26]	film	*H. maydis*	strong inhibition	2015	Mater. Lett.
TiO_2/PPIX/Hem [27]	film	*B. subtilis*	88% inactivation 1.7 h	2015	ACS Appl. Mater. Interfaces
PMMA/TiO_2 [28]	film	*E. coli*	maximal inhibition zone diameters of 14±0.51 mm	2015	Photochem. Photobiol. Sci.
PANI@TiO_2/GN [29]	10 mg $well^{-1}$	*E. coli*	maximal inhibition zone diameters of 17 mm	2016	RSC Advances
CuTCPP-TSI [30]	20 mg mL^{-1}	*E. coli*	99.9% inactivation 3 h	2018	J. Magn. Magn. Mater.
TiO_2@4Si-Ce6-PEG [31]	10 umol/L	*E. coli*	2 log inactivation 3 h	2019	World J. Appl. Chem
F_2POH@qTiO_2 [32]	1.0 mg mL^{-1}	*S. aureus*	3-4 log inactivation 2 h	2019	Catalysts
PANI-TiO_2 [33]	coating	*E. coli*	70% inactivation 0.5 h	2019	Synth. Met.
CuPc/TiO_2 [34]	fabric	*E. coli*	100% inactivation 6 h	2019	Chem. Eng. J.
P_3-TiO_2 [35]	film	*S. aureus*	80.4% inactivation 3 h	2019	Int. J. Mol. Sci.
CMP/TiO_2 [36]	1.0 mg mL^{-1}	*S. aureus*	100% inactivation 6 h	2021	Mater. Sci. Eng. C
TcPcZn−TiO_2 [37]	film	*S. aureus*	76.5% inactivation 0.5 h	2021	ACS Omega
IDT-COOH/TiO_2 (this work)	0.4 mg mL^{-1}	*S. aureus*	100% inactivation 1.5 h 7 log inactivation 2 h		

References

[1] B. Muktha, D. Mahanta, S. Patil, G. Madras, Synthesis and photocatalytic activity of poly(3-hexylthiophene)/TiO_2 composites, J. Solid State Chem. 180 (2007) 2986-2989.

[2] H. Liang, X. Li, Visible-induced photocatalytic reactivity of polymer–sensitized titania nanotube films, Appl. Catal. B-Environ. 86 (2009) 8-17.

[3] D. Wang, J. Zhang, Q. Luo, X. Li, Y. Duan, J. An, Characterization and photocatalytic activity of poly(3-hexylthiophene)-modified TiO_2 for degradation of methyl orange under visible light, J. Hazard. Mater. 169 (2009) 546-550.

[4] Y. Zhu, Y. Dan, Photocatalytic activity of poly(3-hexylthiophene)/titanium dioxide composites for degrading methyl orange, Sol. Energ. Mat. and Sol. C. 94 (2010) 1658-1664.

[5] S. H. Xu, S. Y. Li, Y. X. Wei, L. Zhang, F. Xu, Improving the photocatalytic performance of conducting polymer polythiophene sensitized TiO_2 nanoparticles under sunlight irradiation, Reac Kinet Mech Cat. 101 (2010) 237-249.

[6] Y. Zhu, S. Xu, D. Yi, Photocatalytic degradation of methyl orange using polythiophene/titanium dioxide composites, React. Funct. Polym. 70 (2010) 282-287.

[7] S. Xu, Y. Zhu, L. Jiang, Y. Dan, Visible light induced photocatalytic degradation of methyl orange by polythiophene/TiO_2 composite particles, Water Air Soil Pollut. 213 (2010) 151-159.

[8] S. Xu, L. Jiang, H. Yang, Y. Song, Y. Dan, Structure and photocatalytic activity of polythiophene/TiO_2 composite particles prepared by photoinduced polymerization, Chinese J. Catal. 32 (2011) 536-545.

[9] S. Xu, L. Gu, K. Wu, H. Yang, Y. Song, L. Jiang, Y. Dan, The influence of the oxidation degree of poly(3-hexylthiophene) on the photocatalytic activity of poly(3-hexylthiophene)/TiO_2 composites, Energ. Mat. and Sol. C. 96 (2012) 286-291.

[10] N. Khalfaoui-Boutoumi, H. Boutoumi, H. Khalaf, B. David, Synthesis and characterization of TiO_2-montmorillonite/polythiophene-SDS nanocomposites: application in the sonophotocatalytic degradation of rhodamine 6G, Appl. Clay Sci. 80-81 (2013) 56-62.

[11] J. H. Huang, M. A. Ibrahem, C. W. Chu, Interfacial engineering affects the photocatalytic activity of poly(3-hexylthiophene)-modified TiO_2, RSC Adv. 3 (2013) 26438.

[12] Y. Bai, P. Y. Luo, P. Q. Wang, J. Y. Liu, Z. Fan, G. D. Zhang, Z. W. Qian, Studies on preparation and photocatalytic performance of polythiophene/TiO_2 composite nanoparticles, Asian J. Chem. 25 (2013) 3369-3372.

[12] R. Jamal, Y. Osman, A. Rahman, A. Ali, Y. Zhang, T. Abdiryim, Solid-state synthesis and photocatalytic activity of polyterthiophene derivatives/TiO_2 nanocomposites, Materials. 7 (2014) 3786-3801.

[13] M. Ravi Chandra, T. Siva Rao, S. V. N. Pammi, B. Sreedhar, An enhanced visible light active rutile titania-copper/polythiophene nanohybrid material for the degradation of rhodamine B dye, Mat. Sci. Semicon. Proc. 30 (2015) 672-681. -

[14] M. R. Chandra, T. S. Rao, B. Sreedhar, Recyclable Sn-TiO_2/polythiophene nanohybrid material for degradation of organic pollutants under visible-light irradiation, Chinese J. Catal. 36 (2015) 1668-1677.

[15] R. Kalyani, K. Gurunathan, PTh-rGO-TiO_2 nanocomposite for photocatalytic hydrogen production and dye degradation, J. Photoch. Photobio. A. 329 (2016) 105-112.

[16] B. Yao, C. Peng, Y. He, W. Zhang, Q. Zhang, T. Zhang, Conjugated microspheres FeTCPP–TDI–TiO_2 with enhanced photocatalytic performance for antibiotics degradation under visible light

irradiation, Catal Lett. 146 (2016) 2543-2554.
[17] M. R. Chandra, T. S. Rao, H. S. Kim, S. V. N. Pammi, N. Prabhakarrao, I. Manga Raju, Hybrid copper doped titania/polythiophene nanorods as efficient visible light-driven photocatalyst for degradation of organic pollutants, J. Asian Ceram. Soc. 5 (2017) 436-443.
[18] M. R. Chandra, P. Siva Prasada Reddy, T. S. Rao, S. V. N. Pammi, K. Siva Kumar, K. Vijay Babu, Ch. Kiran Kumar, K. P. J. Hemalatha, Enhanced visible-light photocatalysis and gas sensor properties of polythiophene supported tin doped titanium nanocomposite, J. Phys. Chem. Solids. 105 (2017) 99-105.
[19] C. Liu, X. Cui, Y. Li, Q. Duan, A hybrid hollow spheres $Cu_2O@TiO_2$-g-ZnTAPc with spatially separated structure as an efficient and energy-saving day-night photocatalyst for Cr(VI) reduction and organic pollutants removal, Chem. Eng. J. 399 (2020) 125807.
[20] Salah Bassaid, C. Benhaoua, M. Taleb, M. Sahli, A. Dehbi, Physical and chemical properties of composites based on polythiophene and titanium dioxide nanoparticles for photocatalysis, Polym. Sci. Ser. B. 63 (2021) 291-303.
[21] C. Liu, Y. Li, X. Cui, C. Liang, G. Xing, Q. Duan, Construction of a recyclable dual-responsive TiO_2-based photocatalyst modified with $ZnIn_2S_4$ nanosheets and zinc phthalocyanine for Cr(VI) reduction under visible light, Chem. Eng. J. 417 (2021) 129332.
[22] E. S. Tuchina, V. V. Tuchin, TiO_2 nanoparticle enhanced photodynamic inhibition of pathogens, Laser Phys. Lett. 7 (2010) 607-612.
[23] A. Sułek, B. Pucelik, J. Kuncewicz, G. Dubin, J. M. Dąbrowski, Sensitization of TiO_2 by halogenated porphyrin derivatives for visible light biomedical and environmental photocatalysis, Cataly. Today. 335 (2019) 538-549.
[24] W. H. Jeong, T. Amna, Y. M. Ha, M. S. Hassan, H. C. Kim, M. S. Khil, Novel PANI nanotube@TiO_2 composite as efficient chemical and biological disinfectant, Chem. Eng. J. 246 (2014) 204-210.
[25] D. Qiu, K. Liu, Z. Jiao, Q. Huang, H. Shi, M. Li, Quercetin-sensitized TiO_2 film: photocatalytic inhibition of helminthosporium maydis under visible light irradiation, Mater. Lett. 97 (2013) 21-23.
[26] Y. Zhao, Q. Shang, J. Yu, Y. Zhang, S. Liu, Nanostructured 2D diporphyrin honeycomb film: photoelectrochemistry, photodegradation, and antibacterial activity, ACS Appl. Mater. Inter. 7 (2015) 11783-11791.
[27] A. Salabat, F. Mirhoseini, Applications of a new type of poly(methyl methacrylate)/TiO_2 nanocomposite as an antibacterial agent and a reducing photocatalyst, Photochem. Photobiol. Sci. 14 (2015) 1637-1643.
[28] R. Kumar, M. O. Ansari, N. Parveen, M. Oves, M. A. Barakat, A. Alshahri, Mohd. Y. Khan, M. H. Cho, Facile route to a conducting ternary polyaniline@TiO_2/GN nanocomposite for environmentally benign applications: photocatalytic degradation of pollutants and biological activity, RSC Adv. 6 (2016) 111308-111317.
[29] P. Chanhom, N. Charoenlap, C. Manipuntee, N. Insin, Metalloporphyrins-sensitized titania-silica-iron oxide nanocomposites with high photocatalytic and bactericidal activities under visible light irradiation, J. Magn. and Magn. Mater. 475 (2019) 602-610.
[30] P. M. Perillo, F. C. Getz, Dye sensitized TiO_2 nanopore thin films with antimicrobial activity against methicillin resistant *staphylococcus aureus* under visible light, World J. Appl. Chem, 2016, 1, 9-15.

[31] A. Sułek, B. Pucelik, M. Kobielusz, P. Łabuz, G. Dubin, J.M. Dąbrowski, Surface modification of nanocrystalline TiO_2 materials with sulfonated porphyrins for visible light antimicrobial therapy, Catalysts. 9 (2019) 821.
[32] B. Wen, G. I. N. Waterhouse, M. Y. Jia, X. Jiang, Z. M. Zhang, L. Yu, The feasibility of polyaniline-TiO_2 coatings for photocathodic antifouling: antibacterial effect, Synthetic Met. 257 (2019) 116175.
[33] S. Xu, W. Lu, S. Chen, Z. Xu, T. Xu, V. K. Sharma, W. Chen, Colored TiO_2 composites embedded on fabrics as photocatalysts: decontamination of formaldehyde and deactivation of bacteria in water and air, Chem. Eng. J. 375 (2019) 121949.
[34] K. A. D. F. Castro, N. M. M. Moura, F. Figueira, R. I. Ferreira, M. M. Q. Simões, J. A. S. Cavaleiro, M. A. F. Faustino, A. J. D. Silvestre, C. S. R. Freire, J. P. C. Tomé, S. Nakagaki, A. Almeida, M. G. P. M.S. Neves, New materials based on cationic porphyrins conjugated to chitosan or titanium dioxide: synthesis, characterization and antimicrobial efficacy, IJMS. 20 (2019) 2522.
[35] Y. Wu, Y. Zang, L. Xu, J. Wang, H. Jia, F. Miao, Synthesis of high-performance conjugated microporous polymer/TiO_2 photocatalytic antibacterial nanocomposites, Mater. Sci. Eng. C. 126 (2021) 112121.
[36] W. Vallejo, K. Navarro, C. Diaz-Uribe, E. Schott, X. Zarate, E. Romero, Zn(II)-tetracarboxy-phthalocyanine-sensitized TiO_2 thin films as antimicrobial agents under visible irradiation: a combined DFT and experimental study, ACS Omega. 6 (2021) 13637-13646.